Pure appl. geophys. 149 (1997) 299–312
0033-4553/97/020299-14 $ 1.50 + 0.20/0

Pure and Applied Geophysics

The First Version of the $A_{max}(M_W, R)$ Relationship for Kamchatka

A. A. GUSEV,[1] E. I. GORDEEV,[2] E. M. GUSEVA,[1] A. G. PETUKHIN[1] and V. N. CHEBROV[2]

Abstract—To estimate for the first time the typical relation between peak acceleration A_{max}, moment magnitude M_W and hypocentral distance R for Kamchatka, 101 analog strong motion records for 1969–1993 were employed as the initial data set. Records of acceleration and velocity meters were obtained at 15 rock to medium-ground Kamchatkan sites from 33 earthquakes with $M_W = 4.5–7.8$, at $R = 30–250$ km. A_{max} values were determined from ''true'' acceleration time histories calculated by spectral deconvolution of digitized records. The maximum value over the two horizontal components was used as the A_{max} value in the further analysis. With the scarce data available, there were no chances to determine reliably the whole $A_{max}(M_W, R)$ average surface; thus the shape of this trend surface was determined on a theoretical basis and only the level was fitted to the data. The theoretical model employed included: (1) source spectrum: according to the Brune's spectral model; (2) point-source attenuation: as $1/R$ plus loss specified by $Q(f) = 250\, f^{0.8}$; (3) finite-source correction for a disc-shaped incoherent source, its size depending on M_W; (4) accelerogram duration: including source-dependent and distance-dependent terms; (5) A_{max} value: based on random process representation. Distance trends calculated with this model agree with the empirical ones of FUKUSHIMA and TANAKA (1990). To calculate the absolute level for these trends, observed $A_{max}(M_W, R)$ values were reduced to $M_W = 8$, $R = 100$ km using the theoretical trends as reference. The median of the reduced values, $A_{max}(8, 100)$, equal to 188 gal. was taken as the absolute reference level for the relation we sought. Note that in the process of data analysis we were forced to entirely reject relatively abundant data of two particular stations because of their prominent local amplification ($\times 5.5$) or deamplification ($\times 0.45$).

Key words: Peak acceleration, moment magnitude, hypocentral distance, Kamchatka.

Introduction

The Kamchatka Peninsula and its surroundings are in a region of very high seismic potential, with abundant strong earthquakes. During the last 30 years, a small network of strong motion recording instruments has operated here. Several isolated strong motion records and spectra have been published (FEDOTOV *et al.*, 1973; SHTEINBERG *et al.*, 1975; MOLOTKOV, 1987; GUSEVA *et al.*, 1989; ZOBIN *et al.*, 1988; GUSEV, 1990). In the present paper we analyze, for first time, the bulk of

[1] Institute of Volcanic Geology and Geochemistry, Russian Acad. Sci., 9 Piip blvd., Petropavlovsk-Kamchatsky, Russia, 683006. E-mail: seis@volgeo.kamchatka.su

[2] Kamchatka OMSP, Russian Acad. Sci., 9 Piip blvd., Petropavlovsk-Kamchatsky, Russia, 683006. E-mail: gord@omsp.kamchatka.su

data obtained during these observations. Our first objective was to collect usable data of the network, to digitize analog records and to reconstruct ''true'' acceleration time histories. Thereafter the data analysis proper was carried out. We confined our research to an analysis of horizontal peak accelerations only. This is a first stage in the study of regional data, to be continued elsewhere. Our second objective was to determine, in the first approximation, the relation between peak acceleration, moment magnitude and distance, specific for the Kamchatka region.

The records analyzed in this study have been accumulated by the efforts of several seismological organizations, namely by the Institute of Physics of the Earth (IPE) of the Academy of Science of the USSR (AS USSR), under V. V. Shteinberg, by the Pacific Seismic Expedition of IPE under S. A. Fedotov, by the seismic station ''Petropavlovsk'' of IPE under L. G. Sinelnikova, by the Institute of Volcanology of the Far Eastern Branch of the AS USSR under V. D. Theophilaktov and by Kamchatka Experimental-Methodical Seismic Party under E. I. Gordeev and V. P. Mityakin.

The Strong Motion Network and Recording

Seismic activity of Kamchatka is concentrated mainly around its eastern coast (including Commander Islands and their vicinity). This fact determined the manner in which the strong motion instruments were distributed (Fig. 1). Population density here is very low. The instruments are installed in most of the inhabited points of the eastern coast of Kamchatka and the Commander Islands, including lighthouses, meteorological stations, etc. Many of the instruments are colocated with regional seismic stations. The general location of the instruments is shown in Figure 1. The types of ground at the stations were classified in terms of the standard Russian ground classification that uses three types/''categories'' - I, II and III, corresponding practically to rock, firm ground/stiff soil and soft ground or soil. All instruments are installed on the rock (category I) or medium (category II) ground. Their coordinates and ground conditions are listed in Table 1.

The recording network uses the following types of instruments (all operating in waiting mode): optical-recording accelerometers UAR (an outdated paper-recording type, out of use since 1982), SSRZ (35 mm film, mostly phased out), ASRZ-2, SSRZ-M and ASZ-2 (all three with 70 mm film); and also low-magnification galvanometric velocity meters of the type ISO-2 (35 mm film). The accelerometers are three-component (UAR, SSRZ-M, ASRZ-2, ASZ-2) or four-component (SSRZ) instruments. An additional component records horizontal motion with larger/lower magnification. They use unbalanced torsion sensitive elements with oil (SSRZ) or electromagnetic (other accelerometers) damping ($T = 0.04–0.05$ s, $D = 0.6–0.8$). Typical sensitivity is 20 mm/g for main and 50 mm/g for sensitive channels. An ISO-2 velocity meter is a galvanometric system that employs S-5-S

type 5-s pendulum with a free movement range of 1 cm and GB-120 galvanometers with 0.008 s period. Film speeds are 5–10 mm/s. With the only exception of UAR, time marks are recorded as well. All the instruments are routinely checked and, if required, recalibrated or replaced. Technical and organizational problems of instrument maintenance prevented really permanent operation of the instruments, especially in the early years, therefore the data coverage is not exhaustive, though nearly complete after 1982. At any rate, in 1962–1980 the network recorded each of the three largest ($M_W = 7.6–7.8$) Kamchatka earthquakes of the 30-year period. In 1980–1993 several records of significant earthquakes with magnitudes 6.9–7.2 were obtained.

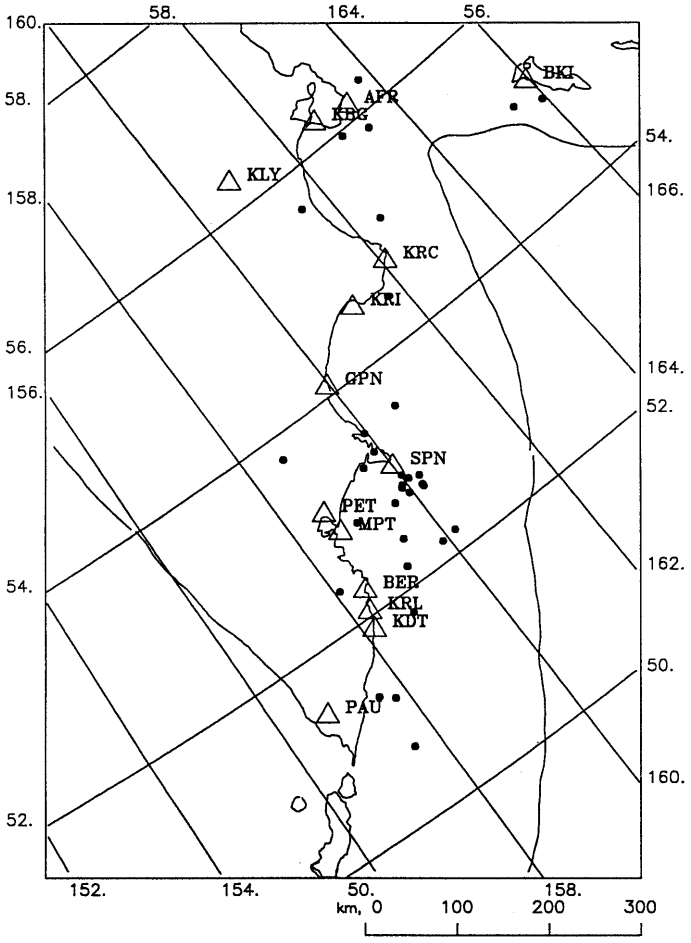

Figure 1
Strong-motion instruments network of Kamchatka. Triangles: instruments (see Table 1). Dots: epicenters of earthquakes given in Table 2.

Table 1

Instrument location and ground conditions

Station name	Code	Lat.	Long.	Ground type	Ground category
Bering	BKI	55.2	166.0	sandstone	rock
Cape Afrika	AFR	56.2	163.4	gravel	medium
Krutoberegovo	KBG	56.3	162.7	gravel	medium
Kronoki	KRI	54.6	161.2	alluvium	medium
Zhupanovo	GPN	54.1	160.0	lava flow	rock
Shipunskiy	SPN	53.1	160.0	green shist	rock
Petropavlovsk Lighthouse	PET	53.0	158.6	gabbro	rock
Petropavlovskiy	MPT	52.9	158.7	–	rock
Aerological st.	AER	53.1	158.6	–	medium
Paratunka	PRT	53.6	158.4	alluvium	medium
Institute	I-V	53.1	158.6	pyroclastic	medium
Mt. Mishennaya	MSN	53.0	158.6	–	rock
Nikolskaya	NKS	53.0	158.6	–	rock
Berezovaya	BER	52.3	158.5	–	rock
Cape Kruglyi	KRL	52.1	158.3	–	rock
Khodutka	KDT	51.9	158.2	–	rock

The Processing of Strong Motion Records

The data processing procedure applied to the records consisted of the following steps.

1. Digitization of optical records by a hand-operated optical-mechanical digitizer (F004 system, typically, 80 counts per second) or, for recent data, using a 300-dpi optical scanner and semi-automatic digitization code, interactively controlled at a computer display.
2. Zero-line correction.
3. Fourier transform.
4. High-pass and low-pass filtering (zero-phase) with adjustable cutoff frequencies, typically set at 0.1 Hz and 20 Hz, respectively.
5. Instrument response correction producing ''true'' acceleration spectrum.
6. Inverse Fourier transform giving acceleration time history.
7. $A_{\max}$ determination.

The software that realizes stages 2–7 was designed by two of the authors in 1978–1980; it was systematically employed in research projects and checked many times, including a few comparisons with the results of independent processing; its detailed description was published earlier (GUSEVA *et al.*, 1989). The program for interactive digitization of scanned records was designed by D. V. Droznin.

The described procedure was applied to 101 horizontal strong motion components, recorded from 33 earthquakes with $M_W = 4.5–7.8$, at hypocentral distances

$R = 30-250$ km. Figure 2 shows the distribution of processed records over magnitude and distance. Epicentral locations are given in Figure 1. Earthquake parameters are summarized in Table 2. For major earthquakes, the M_W estimates mostly are based on compilation (ZOBIN *et al.*, 1988), mainly from surface-wave studies. For smaller events, M_W values used are (in the order of preference): from Harvard CMT solution, estimated from M_{LH} or another surface-wave magnitude, or, if no long- or medium-period data were available, estimated from the regional ''energy class'' short-period magnitude K_S. To make conversions needed in the latter two cases, the empirical nonlinear intermagnitude relationships of GUSEV (1991) (specific for the region under study) were used. In Table 3 we give parameters of the records and also the values of peak acceleration (maximum among two horizontal components). This table is the main result of the first part of the present study.

The Theoretical Model of Dependence of Peak Acceleration on Magnitude and Distance

In regions with a sufficiently large volume of recorded strong motions, the average dependence of peak acceleration on distance, magnitude and other parameters is usually determined based on a purely empirical or semi-empirical basis, using various versions of the multiple regression procedure. In our case however, the data are scarce and such an approach cannot produce reliable results. Instead, we

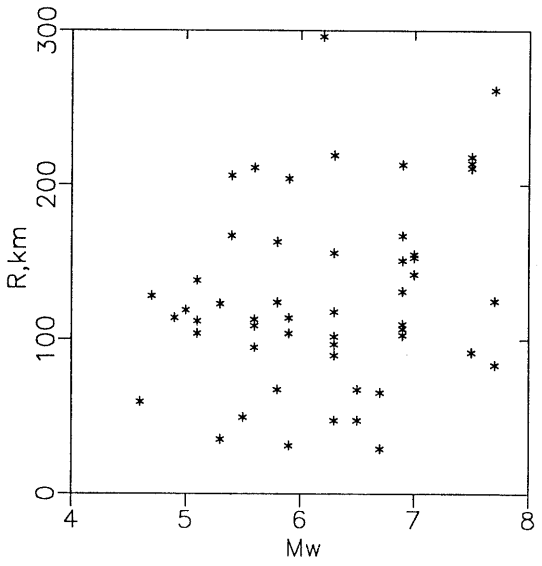

Figure 2
Distribution of processed records over magnitude and distance.

Table 2

List of recorded earthquakes

Date YY.MM.DD	T_0 HH.MM.SS	Epicenter Lat.	Epicenter Long.	H km	Magnitudes M_{LH}	Magnitudes M_S	Magnitudes K_S	Magnitudes M_W*
69.11.22	23.09.35	57.76	163.75	30	7.7	7.3	14.4	7.7 t
71.11.24	19.35.49	52.77	159.66	100	7.2	na	16.0	7.7 z
71.12.15	08.29.55	55.85	163.35	25	7.8	7.8	16.0	7.7 z
71.12.19	07.50.23	55.95	162.90	0	5.8	5.3	11.9	5.9 l
73.03.12	19.39.21	50.80	157.20	70	na	na	14.4	6.7 k
75.07.11	05.23.22	53.23	159.60	115	na	na	11.7	5.0 k
77.11.06	02.39.38	53.50	159.96	60	4.6	na	13.2	5.3 h
77.12.21	16.39.36	52.19	159.90	39	5.3	5.0	12.8	5.6 h
79.06.25	18.45.52	52.74	160.20	31	4.0	na	13.1	4.7 l
80.02.11	15.29.47	53.30	159.90	57	na	na	12.7	5.6 k
80.11.23	15.45.03	52.44	159.42	20	na	na	11.8	5.1 k
80.12.04	10.46.27	52.21	160.17	26	5.6	5.2	12.8	5.4 h
81.02.09	19.31.30	54.94	165.94	20	5.1	4.9	12.2	5.3 h
81.06.25	01.47.56	52.85	159.90	42	4.2	4.3	12.5	4.9 l
81.10.13	15.54.02	51.30	157.60	101	na	na	13.0	5.4 h
82.03.08	15.16.31	52.89	160.08	38	4.2	na	12.1	5.1 h
82.04.17	10.27.12	54.44	161.72	42	na	na	10.9	4.6 k
82.05.14	03.37.58	52.20	159.20	121	na	na	11.9	5.1 k
82.05.31	10.21.21	55.07	165.48	56	6.5	6.4	14.7	6.5 h
82.11.14	08.29.20	52.84	158.98	91	na	na	13.2	5.6 h
83.04.04	19.04.23	52.95	160.02	40	5.7	5.5	13.3	5.9 h
83.07.24	23.07.30	53.77	158.62	180	5.4	na	14.3	5.6 h
83.08.05	00.33.47	52.87	159.93	41	4.7	4.7	12.6	5.5 h
83.08.17	10.55.55	55.64	161.52	98	6.8	6.7	15.0	7.0 h
84.12.28	10.37.47	56.28	163.77	5	7.5	7.0	14.5	6.7 h
85.03.06	22.31.52	55.09	162.48	46	6.0	5.4	14.3	5.9 h
85.05.19	08.07.48	53.54	160.65	40	5.6	na	13.7	5.8 h
87.02.24	07.40.09	52.38	158.08	126	4.0	na	12.8	4.7 l
87.10.06	20.11.36	52.85	160.25	34	6.6	6.3	13.9	6.5 h
92.03.02	12.29.38	52.76	160.20	20	7.1	6.8	14.6	6.9 h
92.03.05	14.39.11	52.77	159.95	31	6.2	6.1	14.0	6.3 h
93.06.08	13.03.37	51.20	157.80	40	7.4	7.3	14.9	7.5 h
93.11.13	01.18.07	51.79	158.83	40	7.1	7.0	14.6	7.0 h

* M_W values are from different sources, and each source is marked by the letter: *t*—tsunami magnitude of ABE (1979); *z*—based on surface-wave and body-wave M_0 estimates summarized in ZOBIN *et al.* (1988); *l*—estimated from M_{LH} based on correlation (GUSEV, 1991); *h*—calculated from M_0 estimate of Harvard CMT.

determined this entire dependence based on a theoretical basis and then only adjusted its absolute level (that is, the coefficient) to the data. Practically, the equivalent procedure was applied: data were reduced to a fixed distance and magnitude and then averaged.

The program realizing the theoretical model (see Fig. 3 for its flow chart) consists of three modules: (1) estimation of the Fourier acceleration spectrum; (2)

Table 3

Peak ''true'' horizontal accelerations

Date YY.MM.DD.	Station code	Instr. type	Δ km	*R* km	M_W	A_{max} cm/s/s
69.11.22	BKI	ISO	260	261	7.7	6.84
71.11.24	PET	ISO	120	125	7.7	90.2
71.12.15	KBG	UAR	80	84	7.7	51.3
71.12.19	KBG	UAR	32	32	5.9	6.66
73.03.12	PET	ISO	242	252	6.7	5.30
75.07.11	PET	ISO	30	119	5.0	0.80
77.11.06	PET	ISO	107	123	5.3	3.35
77.12.21	PET	ISO	70	113	5.6	3.10
79.06.25	PET	ISO	80	128	4.7	2.80
80.02.11	PET	ISO	87	109	5.6	4.75
80.11.23	PRT	ISO	101	104	5.1	2.61
80.12.04	PET	ISO	140	167	5.4	1.86
81.02.09	BKI	SSRZ	30	36	5.3	68.8
81.06.25	PET	ISO	85	114	4.9	2.02
81.10.13	PET	ISO	180	206	5.4	1.13
82.03.08	PET	ISO	110	112	5.1	2.50
82.04.17	KRI	ISO	43	60	4.6	93.4
82.05.14	PET	ISO	66	138	5.1	1.02
82.05.31	BKI	SSRZ	38	68	6.5	33.3
82.11.14	PET	ISO	27	95	5.6	8.65
83.04.04	PET	ISO	90	104	5.9	5.90
83.04.04	KRI	ISO	200	204	5.9	32.1
83.07.24	KRI	ISO	110	211	5.6	37.3
83.08.05	SPN	ISO	29	50	5.5	23.5
83.08.17	KBG	SSRZ	101	153	7.0	192.0
83.08.17	KRI	SSRZ-M	120	155	7.0	231.0
84.12.28	AFR	SSRZ-M	30	30	6.7	185.8
84.12.28	KBG	SSRZ	66	66	6.7	174.0
85.03.06	KRI	ISO	104	114	5.9	55.0
85.05.19	SPN	ISO	55	68	5.8	46.0
85.05.19	I-V	SSRZ	158	163	5.8	14.0
85.05.19	KRI	ISO	117	124	5.8	58.6
87.10.06	SPN	SSRZ-M	34	48	6.5	86.2
92.03.02	KRI	ASZ-2	212	213	6.9	42.5
–	GPN	SSRZ-M	150	151	–	47.1
–	MPT	SSRZ-M	101	103	–	79.4
–	PET	SSRZ-M	105	107	–	25.1
–	MSN	SSRZ-M	108	110	–	90.0
–	BER	ASZ-2	129	131	–	55.6
–	KDT	SSRZ-M	166	167	–	14.6
92.03.05	KRI	ASZ-2	217	219	6.3	21.4
–	SPN	SSRZ-M	36	48	–	42.1
–	MPT	SSRZ-M	85	90	–	68.7
–	AER	SSRZ-M	97	102	–	48.7
–	MSN	SSRZ-M	92	97	–	117.0
–	BER	ASZ-2	114	118	–	21.7
–	KDT	SSRZ-M	153	156	–	11.5

Table 3 (continued)

Date YY.MM.DD.	Station code	Instr. type	Δ km	R km	M_W	A_{max} cm/s/s
93.06.08	AER	SSRZ-M	214	218	7.5	32.8
–	PET	SSRZ-M	208	211	–	29.9
–	NKS	SSRZ-M	208	211	–	40.5
–	MSN	SSRZ-M	211	214	–	101.6
–	KDT	SSRZ-M	83	92	–	220.8
93.11.13	NKS	SSRZ-M	137	142	7.0	108.2
–	PET	SSRZ-M	137	142	–	30.1

estimation of the accelerogram duration; and (3) estimation of A_{max}. The Fourier acceleration spectrum in its turn is a product of three terms: the source spectrum of Brune-Joyner-Boore type (corner frequency plus f_{max}), with the stress drop of 40 bar, $c_S = 3.5$ km/s and $f_{max} = 10$ Hz; the point source attenuation factor that combined $1/R$ geometrical spreading and loss specified by $Q = 250f^{0.8}$ (ABUBAKIROV and GUSEV, 1990); and the source finiteness correction factor calculated for a disc-shaped noncoherent radiator (GUSEV, 1983), with magnitude-dependent disc radius R_S. Note that $1/R$ geometric spreading is a reasonable zero approximation for the behavior of the spectrum of S wave group in Kamchatka region where no L_g group can be observed. The source size L vs. M_0 correlation for Kamchatka was estimated beforehand; it was found to be near the world average trend of the type $L \propto M_0^{0.33}$ (KANAMORI and ANDERSON, 1975); in particular we assumed $\log L = 0.5\, M_W - 1.85$ and also $R_S = 0.4\, L$. The duration T_m for a

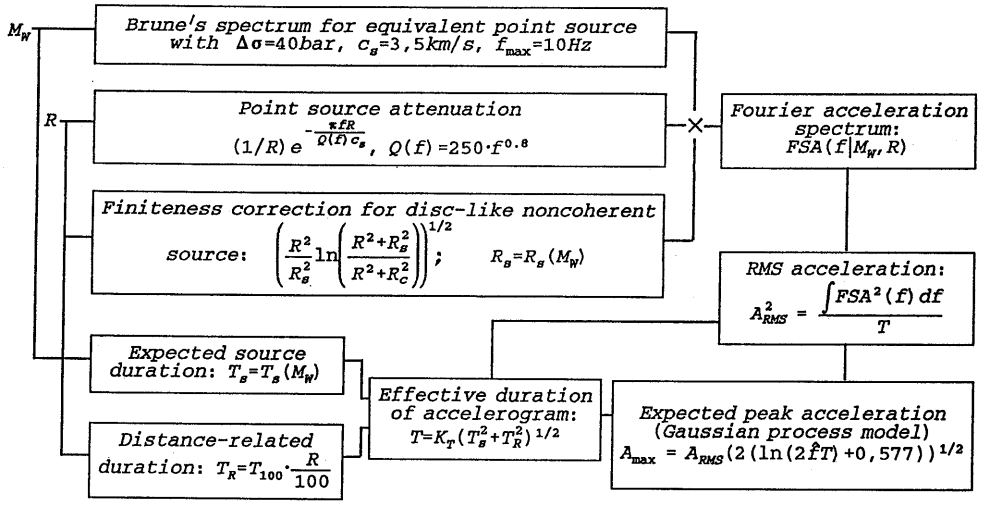

Figure 3
Flow-chart of the theoretical model used to determine the shape of the $A_{max}(M_W, R)$ trend.

maximum part of an accelerogram was calculated as a combination of source-related T_S and distance-related T_R terms, as $T_m = (T_S^2 + T_R^2)^{0.5}$ (GUSEV, 1983). The former is assumed to be equal to $L/3.5$ s for L in km (so that it scales as $M_0^{0.33}$ as well). The latter is assumed to be directly proportional to distance, with a coefficient empirically determined for Kamchatka in advance, based on small earthquake data: $T_R = 3.5(R/100)$ s for R in km. The $A_{\max}$ value was determined based on the Fourier spectrum and duration, following the procedure of GUSEV (1983), mainly similar to that of BOORE (1983). The maximum part of an accelerogram is assumed to follow the model of a segment of the stationary random Gaussian process, and its squared maximum excursion is estimated through mean squared amplitude, determined in its turn by the integral of squared module of the Fourier spectrum over frequency and the value of duration. To additionally check our technique we calculated the distance dependence of peak acceleration for several fixed magnitude values and compared the result with the empirical relation after FUKUSHIMA and TANAKA (1990); the agreement of the attenuation curve shapes (Fig. 6) occurred to be quite reasonable.

Estimation of the Absolute Level of $A_{\max}(M_W, R)$ and Determination of the Average $A_{\max}(M_W, R)$ Dependence for Kamchatka

In order to determine the absolute level of the $A_{\max}(M_W, R)$ dependence we have reduced the observed peak acceleration values to a fixed (M_W, R) combination

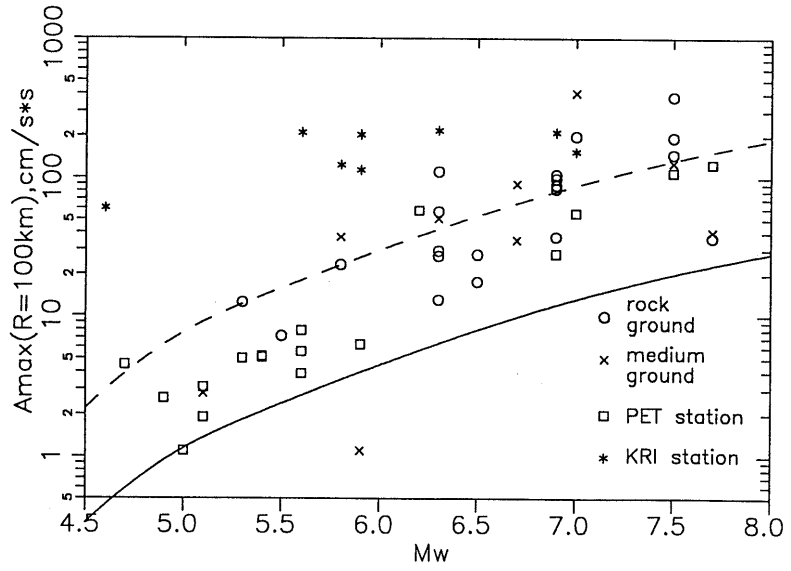

Figure 4
$A_{\max}$ values reduced to $R = 100$ km. Solid line: trend of the theoretical model at $R = 100$ km; dashed line: trend of the accepted $A_{\max}(M_W, R)$ relation for Kamchataka.

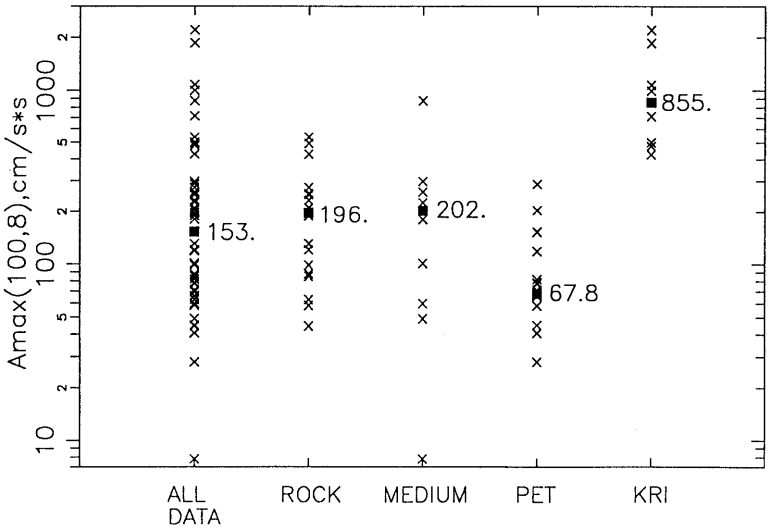

Figure 5
A_{max} values reduced to $M_W = 8$ and $R = 100$ km. The whole data set and four data subsets obtained by various groupings are presented: for PET and KRI stations and for ROCK and MEDIUM ground stations groups, with PET and KRI data excluded. Figures denote median values for each group of data.

by means of the theoretical relation $A_t\,(M_W, R)$ calculated as described above. This was done in two steps: at first the reduction was made to a fixed distance value, which was specified as 100 km; and on the second step the reduction was made to a fixed magnitude value selected as $M_W = 8$. The intermediate result enables one to check whether the magnitude dependence is reasonable. The first step of the reduction can be expressed by the following formula:

$$A_{red}(R = 100) = A_{max}[A_t(M_W, R = 100)/A_t(M_W, R)]. \quad (1)$$

The results of this stage are shown on Figure 4. On the same plot we can see the theoretical curve, calculated according to the described theoretical model. One can see that the general trend of the predicted magnitude dependence is quite consistent with observations, whereas the level (never used), is evidently too low. The second reduction, with respect to magnitude, can be expressed by the following formula:

$$A_{red}(8, 100) = A_{red}(R = 100)[A_t(8, 100)/A_t(M_W, R = 100)]. \quad (2)$$

The results of this step are shown in a graphical form in Figure 5. The reduced data set can be described by the median value of 153 gal. and the standard deviation value of about 0.48 in log (base 10) units (here and below). So large a scatter is unusual: a typical value for the RMS regression residual of log A_{max} data is about 0.25–0.3, much less than our result. Data analysis shows that the effect of ground type is relatively weak, but that a large contribution can be ascribed to the effect of individual stations. In particular, for the reduced data of station PET, the average

log A_{max} value is below the total average by 0.35 (deamplification by 0.45 times). For another anomalous station, KRI, the average reduced log A_{max} is above the total average by 0.74 (amplification by 5.5 times). We discarded data from these two stations despite the fact that they have contributed about 50% of data. (Generally speaking, these data could be station-corrected and in this modification could be useful in some aspects, e.g. in checking the shape of the magnitude dependence of A_{max}; however they are of no use in improving the average value of $A_{max}(8, 100)$ when the station corrections are determined from the same data.) Using data of the remaining stations we determined the median value of reduced acceleration as 188 gal. By chance, contributions of the two anomalous stations approximately compensate one another, and the data median for the edited data is comparable to that of the initial data. The data standard deviation is reduced to 0.4 which is still relatively large.

The value of $A_{max}(M_W = 8,\ 100\ \text{km}) = 188$ gal, combined with the theoretical model described above, defines the preferred average dependence of peak acceleration vs. magnitude and distance for conditions of the east coast of Kamchatka. One can compare this relation for distances of 30 and 100 km and variable magnitude with an analogous relation for Japan according to KAWASHIMA *et al.* (1986), to FUKUSHIMA and TANAKA (1990) and according to SUGITO (1986), as well as with one for the Western USA according to JOYNER and BOORE (1982) (Fig. 7). The values of JMA magnitude used by Japanese authors were converted to M_W using the relationship given in GUSEV (1991). One can see that the estimated Kamchatka

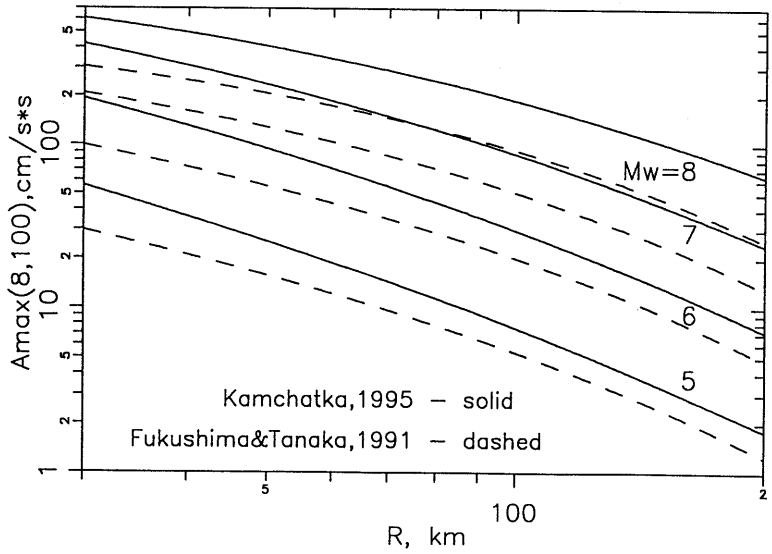

Figure 6
Distance dependence of the $A_{max}(M_W, R)$ relationship for several fixed magnitude values as compared to the empirical relationship after FUKUSHIMA and TANAKA (1990).

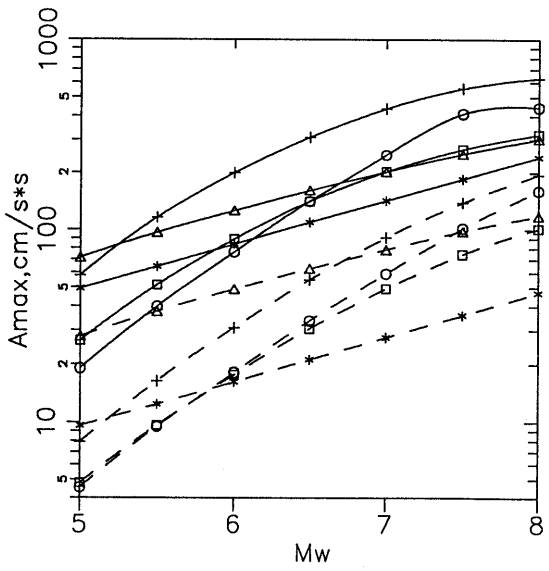

Figure 7
The $A_{max}(M_W, R)$ relationship for Kamchatka (crosses) calculated for two fixed distances 30 km (solid lines) and 100 km (dashed lines) with magnitude as a free parameter, in comparison with analogous relationships of KAWASHIMA *et al.* (1986) (triangles), FUKUSHIMA and TANAKA (1990) (squares), SUGITO (1986) (circles) and JOYNER and BOORE (1982) (stars).

average accelerations are slightly above those for Japan, and markedly above those for Western USA.

Rather large residual scatter in the values of reduced acceleration, even after rejection of data of anomalous stations, deserved special attention. At least part of this scatter must be related to an unusual diversity of spectral shapes. On Figure 8 one can see Fourier acceleration spectra of two records obtained on the same station KBG from events of comparable magnitude and distance. The difference between f_{max} values is about four times; this leads to a large difference between reduced accelerations (by 2 times).

This example is interesting also from the point of view of the source spectrum theory. It illustrates the situation when the f_{max} is likely to be formed (for the lower-frequency source) by source processes. Another alternative is to attribute the difference to the difference between propagation paths. These paths include the near-surface low-Q layer under the station, which is common to both paths and definitely cannot produce such an effect, and also the remaining (main) part of the propagation path. The effect of differences between main parts of propagation paths cannot be excluded, but seems quite unlikely because, to produce a spectral difference in this way, a Q decrease of several times combined with the very unusual shape of $Q(f)$ relationship is needed along the propagation path to the 1971 event.

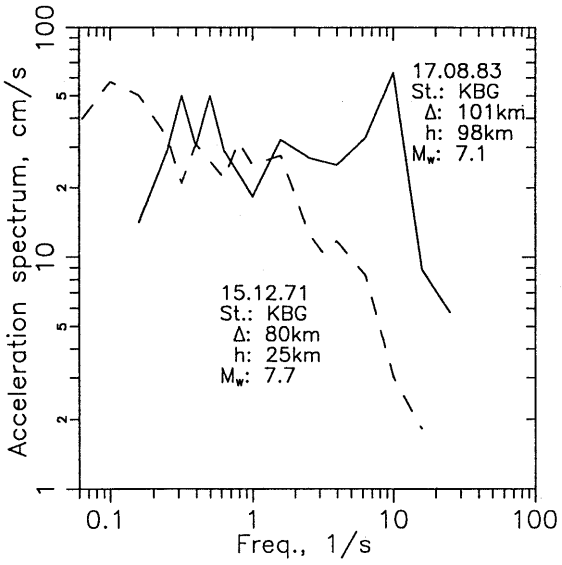

Figure 8
Sample Fourier acceleration spectra of two records with different f_{max} obtained at the same station KBG.

No evidence of significant attenuation anomalies has ever been found during detailed studies of small earthquakes in this region.

Conclusions

1. The data base of 101 digitized Kamchatka strong motion data has been created.

2. These data have been processed giving ''true'' acceleration and A_{max} values.

3. Using the original data reduction scheme, a first version of average $A_{max}(M_W, R)$ relationship for Kamchatka is determined.

4. Prominent individual station anomalies and source spectral diversity are found resulting in unusually wide data scatter around the average $A_{max}(M_W, R)$ relationship.

REFERENCES

ABE (1979), *Size of Great Earthquakes of 1837–1974 Inferred from Tsunami Data,* J. Geophys. Res. *84,* 1561–1568.

ABUBAKIROV, I. R., and GUSEV, A. A. (1990), *Estimation of Scattering Properties of Lithosphere of Kamchatka Based on Monte-Carlo Simulation of Record Envelope of a Near Earthquake,* Phys. Earth. Planet Interiors *64,* 52–67.

BOORE, D. M. (1983), *Stochastic Simulation of High-frequency Ground Motions Based on Seismological Models of the Radiated Spectra*, Bull. Seismol. Soc. Am. *73*, 1865–1894.

FEDOTOV, S. A., GUSEV, A. A., ZOBIN, V. M., KONDRATENKO, A. M., and CHEPKUNAS, K. E. (1973), *Ozernovskoe earthquake and tsunami of November 22, 1969.* In *Earthquakes in the USSR in 1969* (Nauka, Moscow) pp. 195–208 (in Russian).

FUKUSHIMA, Y., and TANAKA, T. (1990), *A New Attenuation Relation for Peak Horizontal Acceleration of Strong Earthquake Ground Motion in Japan*, Bull. Seismol. Soc. Am. *80*, 757–783.

GUSEV, A. A. (1983), *Descriptive Statistical Model of Earthquake Source Radiation and its Application to Short-period Strong Motion*, Geophys. J. Roy. Astr. Soc. *74*, 787–808.

GUSEV, A. A. (1990), *A preliminary version of design seismic load for Petropavlovsk-Kamchatsky*. In *Voprosy Inzhenernoi Seismologii*, iss. 31 (Nauka, Moscow 1990) pp. 67–85 (in Russian).

GUSEV, A. A. (1991), *Intermagnitude Relationships and Asperity Statistics*, Pure and Appl. Geophys. *136*, 515–527.

GUSEVA, E. M., GUSEV, A. A., and OSKORBIN, L. S. (1989), *A Program Package for Digital Processing of Seismic Records and its Testing Using Some Strong Motion Records*, Vulkanol. Seismol. No. 1, 35–49.

JOYNER, W. B., and BOORE, D. M. (1982), *Prediction of Earthquake Response Spectra*. Open-File Report 82–977, U.S. Geological Survey.

KANAMORI, H., and ANDERSON, D. L. (1975), *Theoretical Basis of Some Emprical Relations in Seismology*, Bull. Seismol. Soc. Am. *65*, 1073–1095.

KAWASHIMA, K., AIZAWA, K., and TAKAHASHI, K. (1986), *Attenuation of Peak Ground Acceleration, Velocity and Displacement Based on Multiple Regression Analysis of Japanese Strong Motion Records*, Earthquake Eng. Struct. Dyn. *14*, 199–215.

MOLOTKOV, S. G. (1987), *Spectrum and polarization of strong motions of Kamchatka Peninsula*. In *Voprosy Inzhenernoi Seismologii*, iss. 28 (Nauka, Moscow 1987) pp. 209–221 (in Russian).

SHTEINBERG, V. V., FREMD, V. D., and THEOPHILAKTOV, V. D. (1975), *Ground motions from large earthquakes on Kamchatka* in 1971. In *Sil'nye Kamchatskie Zemletryaseniya v 1971 Godu* (DVNTs, Vladivostok 1975) pp. 7–14 (in Russian).

SUGITO, M. (1986), *Earthquake Motion Prediction, Microzonation and Buried Pipe Response for Urban Seismic Damage Assessment* (School of Civil Engineering, Kyoto University 1986).

ZOBIN, V. M., FEDOTOV, S. A., GORDEEV, E. I., GUSEVA, E. M., and MITYAKIN, V. P. (1988), *Large Earthquakes in Kamchatka and Commander Islands in 1961–1986*, Vulkanol. Seismol. No. 1, 3–23.

(Received February 13, 1996, accepted June 24, 1996)